Supporting Information

for

Generalized Green Synthesis and Formation Mechanism of Sponge-Like Ferrite Micro-Polyhedra with Tunable Structure and Composition

Guoxiu Tong,[†*] *Fangfang Du*,[†] *Lingjing Xiang*,[†] *Fangting Liu,*[†] *Jiayi Hu*,[†] *and Jianguo Guan*[‡*]

[†]College of Chemistry and Life Science, Zhejiang Normal University, Jinhua 321004, China.

[‡]State Key Laboratory of Advanced Technology for Materials Synthesis and Processing, Wuhan University of Technology, Wuhan 437000, China

[*] Prof. Dr. G. X. Tong

College of Chemistry and Life Sciences, Zhejiang Normal University,

No.688, Yingbin Road, Jinhua 321004 P. R. China

Phone: 86-579-82282269; Fax: 86-579-82282269

E-mail: **tonggx@zjnu.cn**

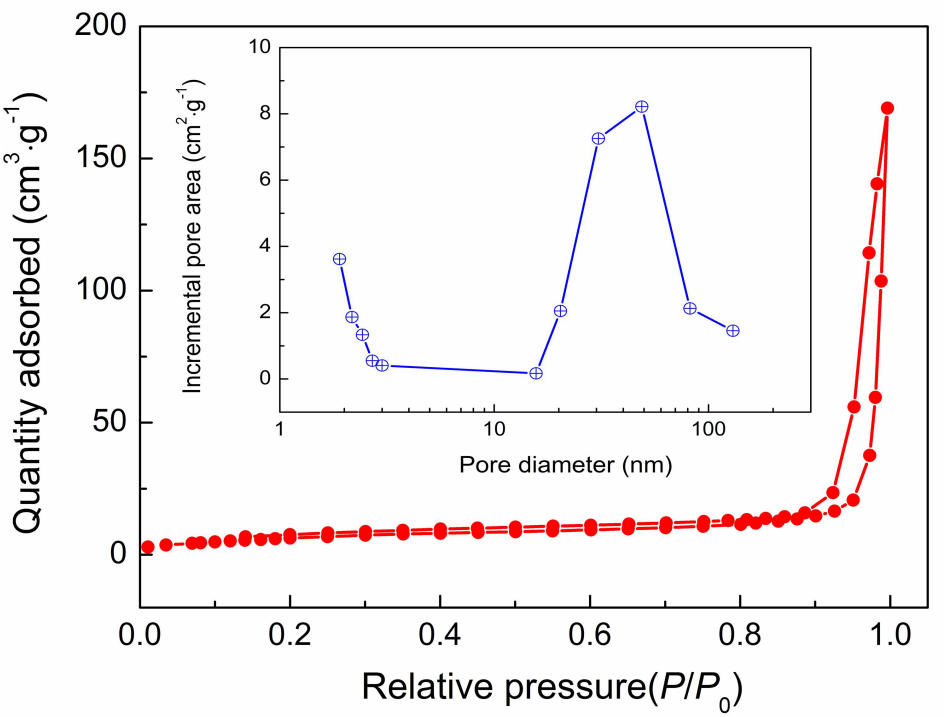

Figure S1. Nitrogen adsorption/desorption isotherms and their corresponding pore size distribution curves (the inset) for the precursors.

The nitrogen physical adsorption/desorption isotherms and the corresponding pore size distribution curves of the precursors are shown in **Figure S1**. As shown in the figure, the precursors demonstrated type IV isotherms with H3 hysteresis loops according to BDDT classification. As expected for the observed porous nature, the typical precursors samples had a low S_{BET} of 24.62 $m^2 \cdot g^{-1}$, with pore volume of 0.058 $m^3 \cdot g^{-1}$ and average pore size of 9.45 nm.

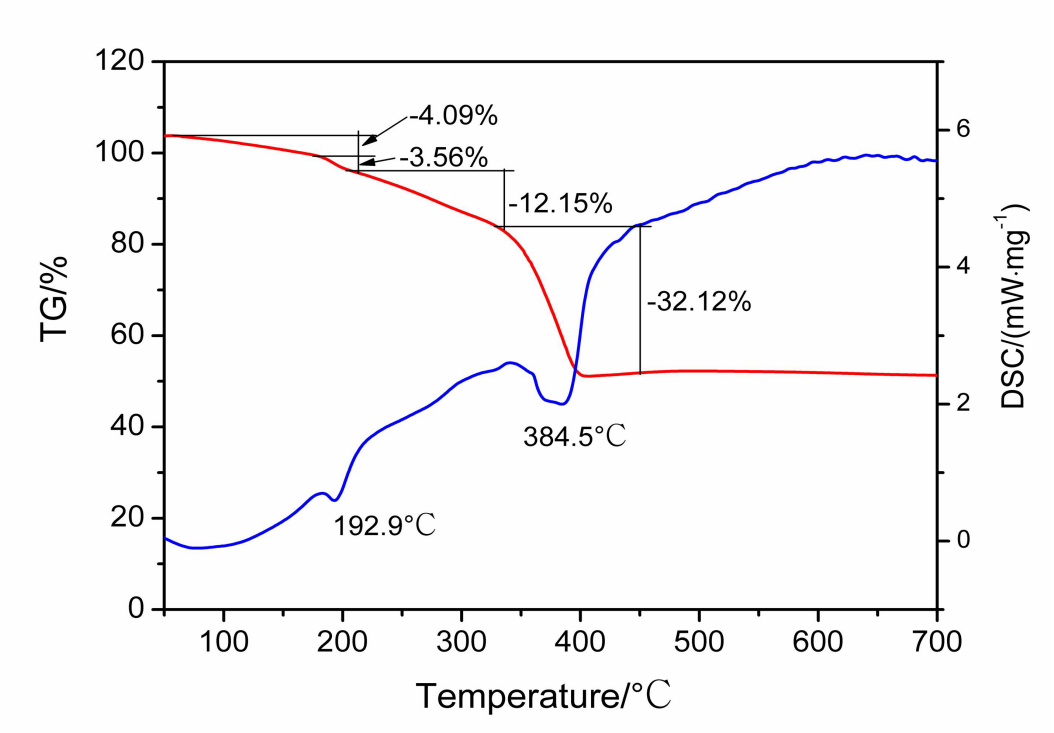

Figure S2. The thermogravimetry–differential scanning calorimetry (TG-DSC) of the precursor heated in air.

The TG-DSC curves of the precursor are shown in **Figure S2**. The small broad endothermic peak below 200 ºC in DSC curve can be assigned to the removal of the free water and constitution water in the precursor, relative to a total mass loss of 7.56% in TG curve. The oxidative decomposition of the precursor was indicated by the presence of the broad exothermic peak over 200 to 384 °C, which corresponds to a weight loss of 44.27 %. The weight was kept unchanged after 400 °C, meaning the stable composition. The exothermic peak after 400 °C is due to the phase transformation of the resultant products. The result implies that the organic matter can be removed by sintering at 350 °C for longer time.

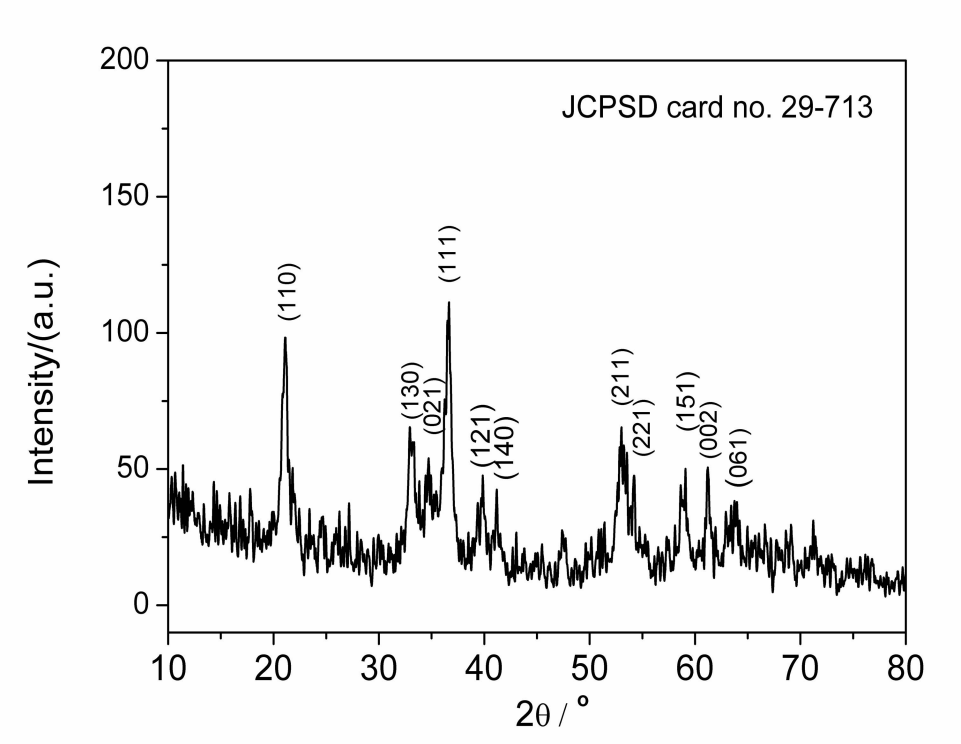

Figure S3. XRD pattern of the precursors formed in the absence of glucose.

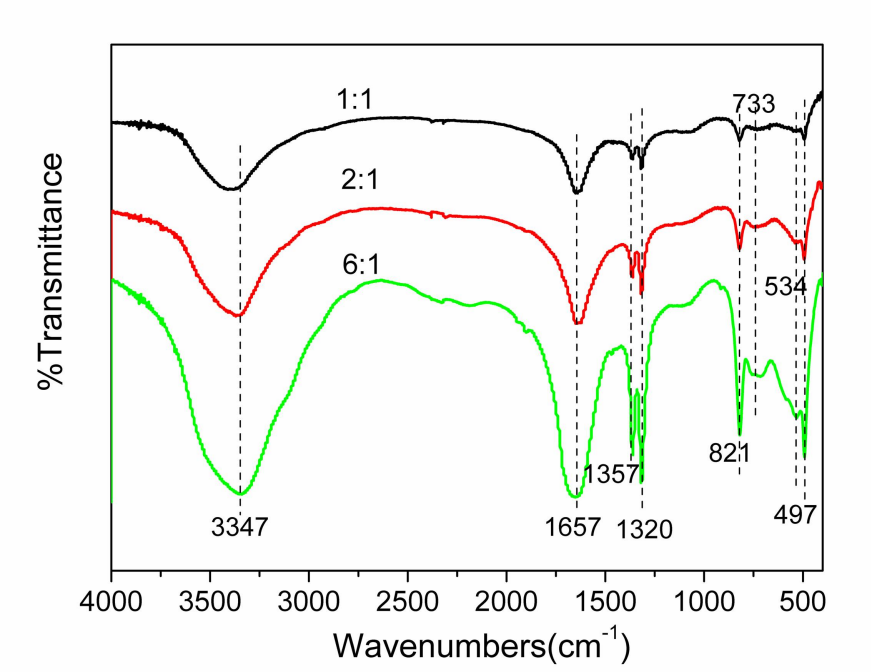

Figure S4. IR spectra of the precursors formed at various molar ratios of glucose to Fe^{3+}.

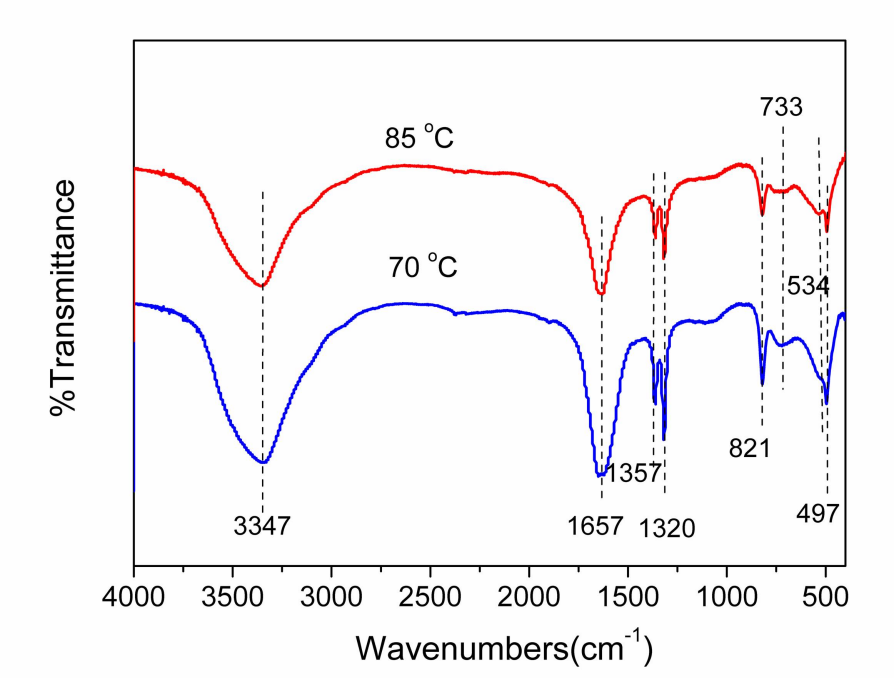

Figure S5. IR spectra of the precursors formed at various temperatures.

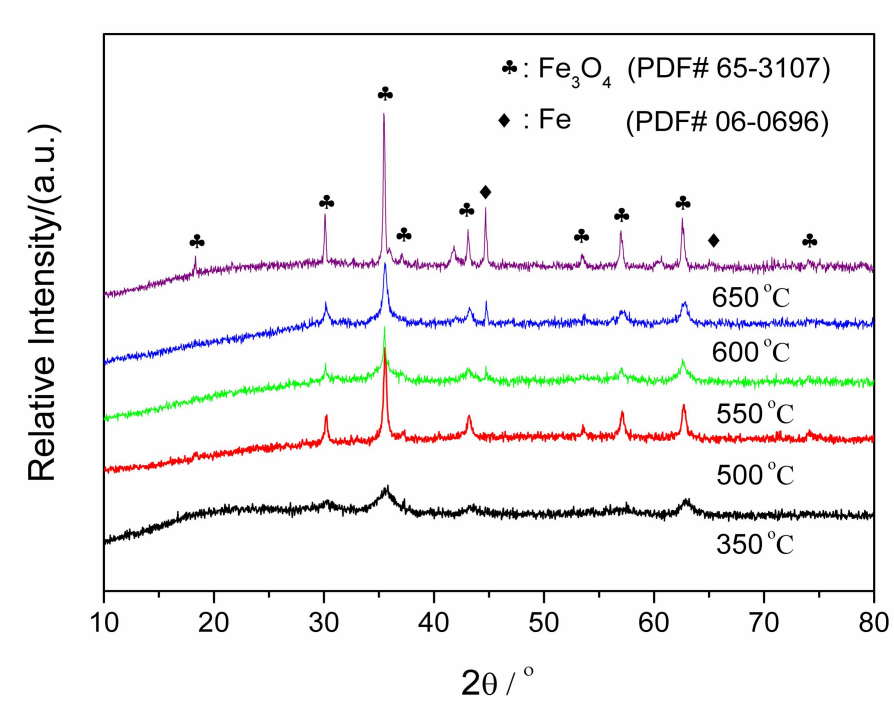

Figure S6. XRD patterns of the samples obtained by annealing the precursors at various temperatures for 3 h under N_2. The precursor is obtained with the glucose /iron nitrates molar ratio of 1:3.

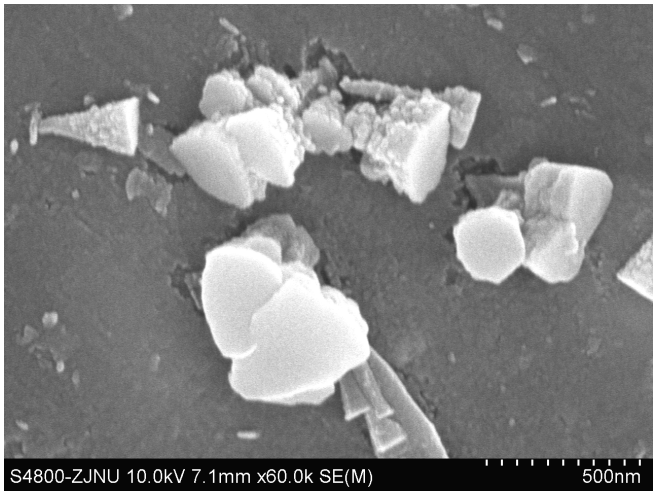

Figure S7. SEM image of the precursors obtained at 2 min after yellow-green sediment appeared.

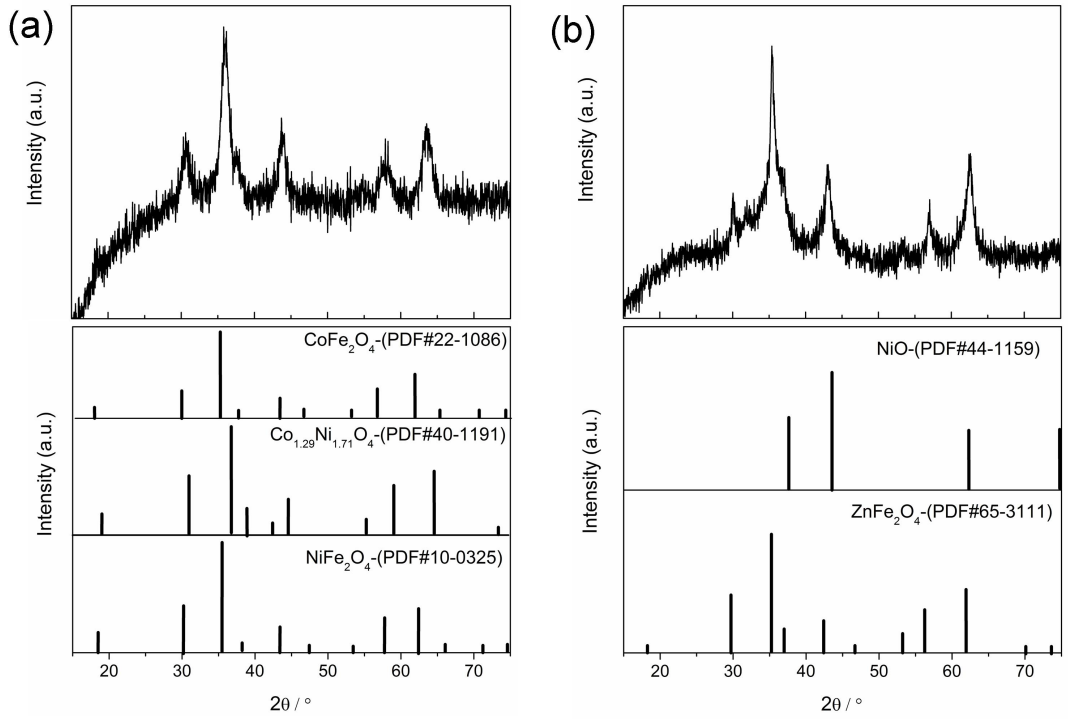

Figure S8. XRD patterns of (a) $CoFe_2O_4/NiFe_2O_4/Co_{1.29}Ni_{1.71}O_4$ hexahedra and (b) $NiO/ZnFe_2O_4$ hexahedra obtained by annealing the corresponding precursors at 500 °C for 3 h. The precursors in (a) is obtained with the glucose/ nitrates molar ratio of 1:3 and $Co^{2+}/Ni^{2+}/Fe^{3+}$ molar ratio of 1:1:4. The precursors in (b) is obtained with the glucose/ nitrates molar ratio of 1:3 and $Zn^{2+}/Ni^{2+}/Fe^{3+}$ molar ratio of 1:1:4.

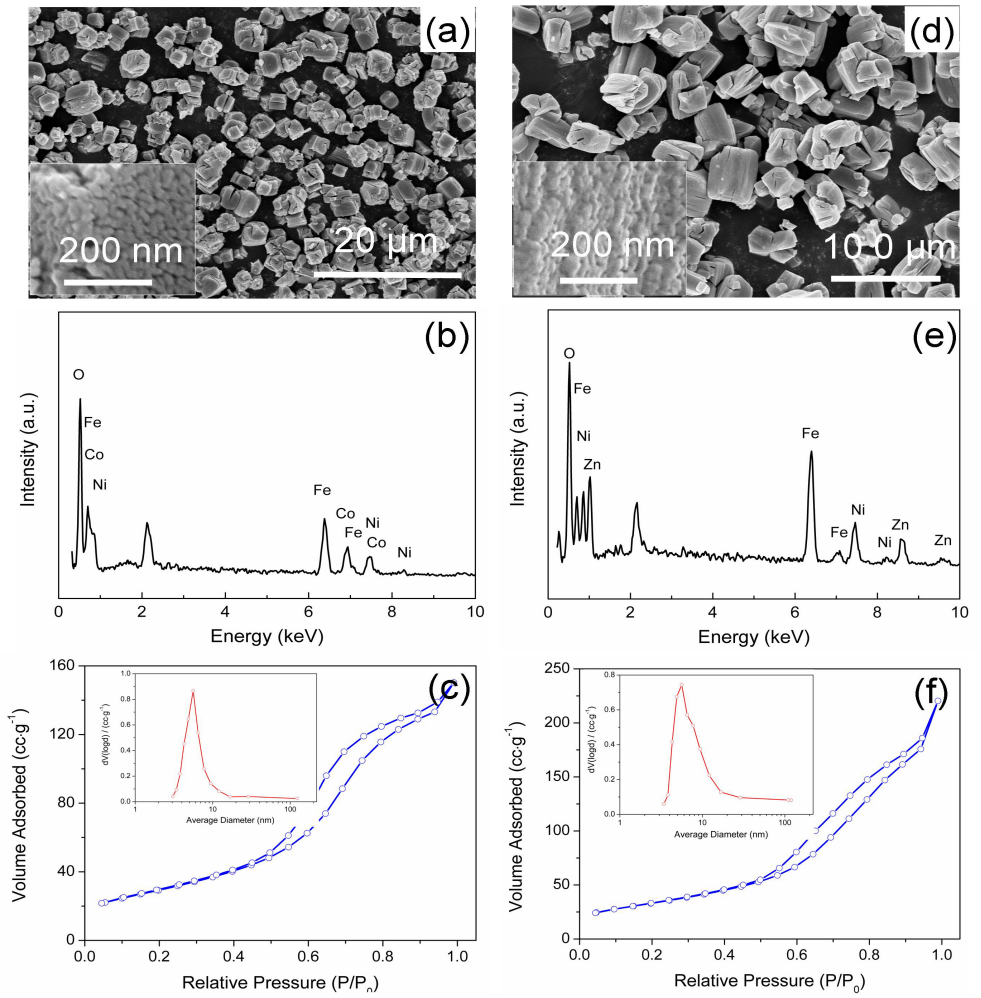

Figure S9. (a and d) SEM images, (b and e) EDX patterns, and (c and f) nitrogen adsorption/desorption isotherms and the corresponding pore size distribution curves (inset) of the samples obtained by annealing the precursors at 500 °C for 3 h. The samples in (a, b, and c) corresponds to $CoFe_2O_4$/ $NiFe_2O_4$/$Co_{1.29}Ni_{1.71}O_4$ hexahedra, and their precursors are formed at the glucose/ nitrates molar ratio of 1:3 and Co^{2+}/Ni^{2+}/Fe^{3+} molar ratio of 1:1:4. The samples in (d, e, and f) corresponds to NiO/$ZnFe_2O_4$ hexahedra, and their precursors are obtained with the glucose/ nitrates molar ratio of 1:3 and Zn^{2+}/Ni/Fe^{3+} molar ratio of 1:1:4.

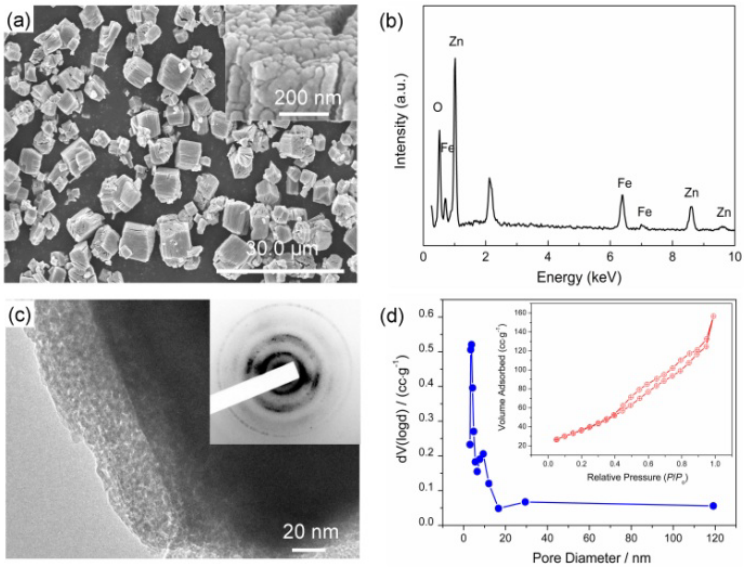

Figure 10. (a) Low-enlarged and high-enlarged (inset) SEM images, (b) EDX spectrum, (c) TEM image and SAED pattern (inset), and (d) nitrogen adsorption/desorption isotherms and the corresponding pore size distribution curves (inset) of spongy $ZnO/ZnFe_2O_4$ micropolyhedra obtained by annealing the precursor at 400 °C for 5 h. The precursor is obtained with the sucrose/nitrates molar ratio of 1:3 and Zn^{2+}/Fe^{3+} molar ratio of 1:2.

Substituting glucose with sucrose can also obtain $ZnO/ZnFe_2O_4$ sponges with regular polyhedral configuration using an admixture of zinc nitrate and iron nitrate as raw materials, followed by sintering at 400 °C for 5 h (Figure S10). The SEM and TEM observations revealed that the products are polyhedral particles ranging from 5 μm to 8 μm in length with aspect ratio of about 1.0. Massive pores and rod-like particles with length of 5 nm to 10 nm are present on these polyhedra, which evolve into sponge-like porous structures (Figures S10a and c). The obscure diffraction rings in the inset of Figure S10c indicated polycrystalline nanoparticles. The EDX analysis (Figure S10b) demonstrated that the Zn/Fe atoms ratio is 1.67, whereas the XRD pattern (Figure S11a) confirmed the existence of two phases, containing ZnO and $ZnFe_2O_4$, according to JCPDS Card Nos. 65-3411 and 65-3111. The nitrogen adsorption/desorption analysis further disclosed that such spongy structures show a high S_{BET} of 135.46 $m^2 \cdot g^{-1}$, bimodal pore-size distribution with pore peaks located at 3.4 and 9.3 nm, pore volume of 0.235 $m^3 \cdot g^{-1}$, and average pore size of 3.38 nm (Figure S10d). Therefore, the as-obtained products were spongy $ZnO/ZnFe_2O_4$ polycrystalline polyhedra.

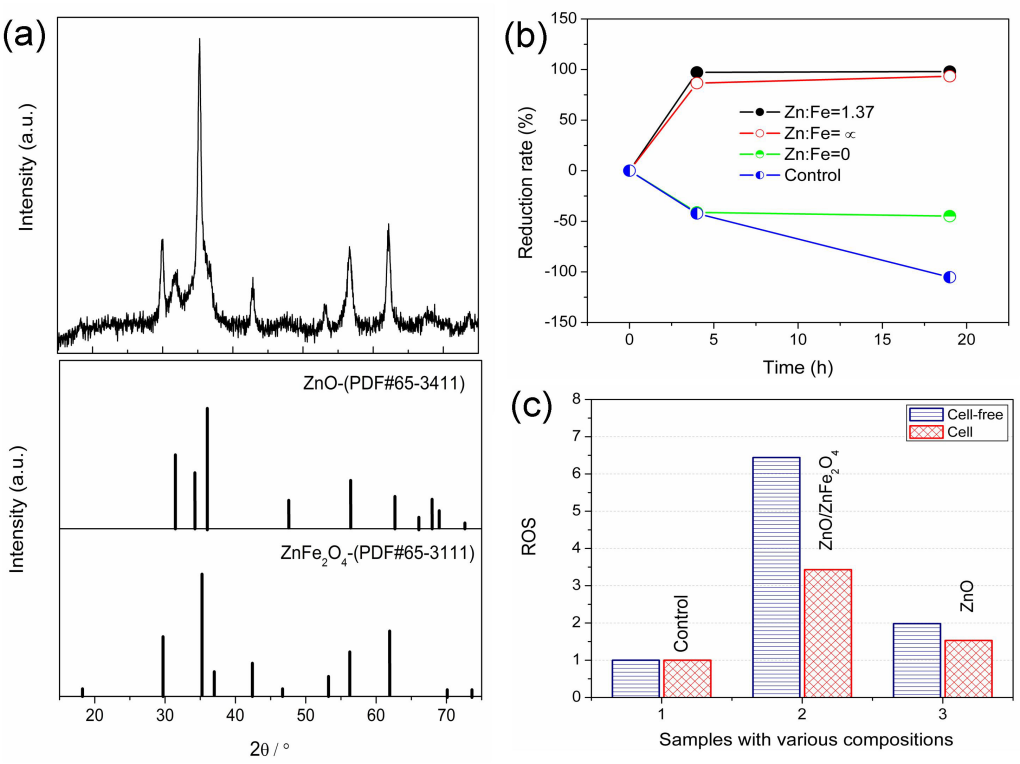

Figure S11. XRD pattern of $ZnO/ZnFe_2O_4$ hexahedra obtained by annealing the precursor at 500 °C for 3 h. The precursor is obtained with the sucrose/ nitrates molar ratio of 1:3 and Zn^{2+}/Fe^{3+} molar ratio of 1:2. (b) Reduction rate of the various samples obtained through ATP test, and (c) ROS (reactive oxygen species) production with and without the presence of the bacterial cells, using the samples without the ZnO and $ZnO/ZnFe_2O_4$ samples as the control.

The antibacterial activities of spongy $ZnO/ZnFe_2O_4$ composites against *Escherichia coli* were obtained through ATP (adenosine triphosphate) test (in Figure S11b). Compared with pure ZnO and Fe_2O_3, the obtained $ZnO/ZnFe_2O_4$ sponges have higher ROS, thereby showing stronger antibacterial activity, with reduction rates ranging between 97.2 % to 98.0 % from 4 h to 19 h (Figures S9b and c in the Supplement Information). The enhanced antibacterial activity is ascribed to the interfacial energy transfer and carrier relaxation across a heterojunction. Further details about the effect of composition, grain size, and surface area of $ZnO/ZnFe_2O_4$ on the antibacterial activity will be reported in our subsequent work.

The bacterial growth was measured via ATP bioluminescence assay according to *Standard Methods for the Examination of Water and Wastewater*[1] with slight modifications using a 3M™ Clean-Trace™ Surface ATP. Briefly, after incubated overnight in LB broth at 37 °C, the bacterial cells were diluted to OD_{600} 0.03 (SHIMADZU UV-1700) using 50 % of the LB broth (diluted by 0.85 % NaCl). 0.03 g

of each ZnO particles (5 types) was placed in a microplate well (Dia 22 mm), following by 3 ml of the bacterial suspension being pipetted into each well. Each treatment was performed in two replicates. The microplates were then sealed using parafilm, mixed gently in order to let cells fully be exposed to the particles and placed under light (3200–3750 lux) in an incubator (37 °C). At the start of the experiment (0 h) and the end (19 h), 20 µL of the bacterial suspensions was pipetted on the ATP swab, and tested of ATP reading (RLU). Bactericidal capability of the ZnO nanoparticles was expressed using reduction rate, calculated via the following equation: reduction rate (%)=(B–A)/B×100% where B and A is the ATP test results before and after 19 h contact, respectively.

ROS generation in solutions containing the ZnO nanoparticles, as well as that within cells upon exposure to the nanoparticles, were determined, according to the methods we previously described.[2] In particular, 2', 7'-diclorofluorescein diacetate (H_2DCF-DA) was used a molecular probe for detecting ROS. For the experiments with the cell-free ZnO suspensions, ROS generation was detected after 30 min under light (2230-2800 Lux). For the experiments with the cells, the bacterial cells was firstly harvested and exposed to 1 % of the PBS solutions containing ZnO nanoparticles and H_2DCF-DA for 40 min in microplates. After sufficient washing of the samples (cells + ZnO nanoparticles), intensity of fluorescent light given off by 2',7'- dichlorofluorescin (DCF) was detected by a microplate reader at 528 nm with 485 nm as excitation wavelength. Triplicates were performed for each treatment.

References

(1) National Committee for Clinical Laboratory Standards. Performance standards for antimicrobial disc susceptibility tests, National Committee for Clinical Laboratory Standards, NCCLS in Villanova, Pa. USA. **1975**.

(2) American Public Health Association. Standard Methods for the Examination of Water and Wastewater, 20th ed. American Public Health Association, Washington, DC, USA. **1998**.